Accepted Manuscript

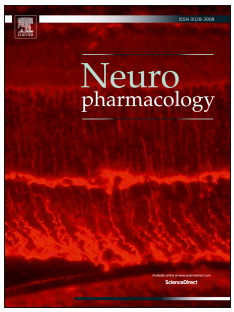

Methamphetamine abstinence induces changes in μ-opioid receptor, oxytocin and CRF systems: Association with an anxiogenic phenotype

Polymnia Georgiou, Panos Zanos, Juan-Antonio Garcia-Carmona, Susanna Hourani, Ian Kitchen, Maria-Luisa Laorden, Alexis Bailey

PII: S0028-3908(16)30047-8

DOI: 10.1016/j.neuropharm.2016.02.012

Reference: NP 6172

To appear in: *Neuropharmacology*

Received Date: 4 November 2015

Revised Date: 14 January 2016

Accepted Date: 14 February 2016

Please cite this article as: Georgiou, P., Zanos, P., Garcia-Carmona, J.-A., Hourani, S., Kitchen, I., Laorden, M.-L., Bailey, A., Methamphetamine abstinence induces changes in μ-opioid receptor, oxytocin and CRF systems: Association with an anxiogenic phenotype, *Neuropharmacology* (2016), doi: 10.1016/j.neuropharm.2016.02.012.

Title page

Methamphetamine abstinence induces changes in μ-opioid receptor, oxytocin and CRF systems: Association with an anxiogenic phenotype

Polymnia Georgiou[a1] (Ph.D), Panos Zanos[a1] (Ph.D), Juan-Antonio Garcia-Carmona[b], Susanna Hourani[a] (Ph.D), Ian Kitchen[a] (Ph.D), Maria-Luisa Laorden[b] (Ph.D), Alexis Bailey[a,c*] (Ph.D)

[a]School of Biosciences and Medicine, Faculty of Health and Medical Sciences, University of Surrey, Guildford, GU2 7XH, Surrey, UK

[b]Department of Pharmacology, School of Medicine, University of Murcia, Spain

[c] Institute of Medical and Biomedical Education, St George's University of London, London SW17 0RE, UK

*Correspondence: Alexis Bailey

Institute of Medical and Biomedical Education
St George's University of London
London SW17 0RE, UK

Tel: +44 (0)1483682564

Fax: +44(0)1483686401

Email: abailey@sgul.ac.uk

[1] Current address: Department of Psychiatry, School of Medicine, University of Maryland, Baltimore, 21201, USA.

Abstract

The major challenge in treating methamphetamine addicts is the maintenance of a drug free-state since they experience negative emotional symptoms during abstinence, which may trigger relapse. The neuronal mechanisms underlying long-term withdrawal and relapse are currently not well-understood. There is evidence suggesting a role of the oxytocin (OTR), μ-opioid receptor (MOPr), dopamine D_2 receptor (D_2R), corticotropin-releasing factor (CRF) systems and the hypothalamic-pituitary-adrenal (HPA)-axis in the different stages of methamphetamine addiction. In this study, we aimed to characterize the behavioral effects of methamphetamine withdrawal in mice and to assess the modulation of the OTR, MOPr, D_2R, CRF and HPA-axis following chronic methamphetamine administration and withdrawal. Ten-day methamphetamine administration (2 mg/kg) increased OTR binding in the amygdala, whilst 7 days of withdrawal induced an upregulation of this receptor in the lateral septum. Chronic methamphetamine treatment increased plasma OT levels that returned to control levels following withdrawal. In addition, methamphetamine administration and withdrawal increased striatal MOPr binding, as well as c-Fos^+/CRF^+ neuronal expression in the amygdala, whereas an increase in plasma corticosterone levels was observed following METH administration, but not withdrawal. No differences were observed in the D_2R binding following METH administration and withdrawal. The alterations in the OTR, MOPr and CRF systems occurred concomitantly with the emergence of anxiety-related symptoms and the development of psychomotor sensitization during withdrawal. Collectively, our findings indicate that chronic methamphetamine use and abstinence can induce brain-region specific neuroadaptations of the OTR, MOPr and CRF systems, which may, at least, partly explain the withdrawal-related anxiogenic effects.

Keywords: methamphetamine withdrawal, oxytocin, μ-opioid receptor, CRF, anxiety

Highlights:

- METH withdrawal induces anxiety-related symptoms in mice
- METH administration and withdrawal causes neuroadaptations in the OT system
- Persistent increase in striatal MOPr following METH treatment
- Amygdalar c-Fos^{+}/CRF^{+} neurons are increased in METH-treated/withdrawn mice

1. Introduction

Methamphetamine (METH) is a potent psychostimulant drug with a high prevalence of worldwide abuse (Eslami-Shahrbabaki *et al.*, 2015). Chronic METH use has been shown to induce emotional impairment including anxiety and depression, as well as psychotic behaviors in humans (see Panenka et al., 2013). Even after long-term abstinence from METH use, former addicts suffer from cognitive and emotional symptoms, which may act as a motivational trigger to re-administer the drug and relapse (Zorick et al., 2010). Currently, there is no effective pharmacotherapy for the treatment of METH addiction.

Although several mechanisms have been suggested, the mechanisms underpinning METH addiction/withdrawal and its behavioral and emotional consequences remain unclear. Recent evidence has implicated the oxytocin (OT) system in the modulation of several METH addiction processes (see McGregor and Bowen, 2012). In particular, pre-clinical studies in rodents showed that intracerebroventricular (i.c.v.) OT administration reduces METH-induced hyper-locomotion (Qi et al., 2008) and intra-nucleus accumbens core (AcbC) oxytocin administration attenuates METH-induced conditioned place preference (CPP) (Qi et al., 2009). Moreover, i.c.v. administration of oxytocin facilitated the extinction of METH-induced CPP and i.c.v. (Qi et al., 2009) as well as intra-hippocampal and intra-medial prefrontal cortex (Han et al., 2014) administration of OT prevented stress-induced reinstatement of METH-seeking. Similarly, intra-AcbC (Baracz et al., 2014), as well as peripheral (Carson et al., 2010; Cox et al., 2013) administration of OT attenuated METH-primed reinstatement in rodents. In addition, Hicks et al. (2014) showed that a 10-day oxytocin administration during adolescence was able to decrease the motivation to self-administer METH and to attenuate priming-induced reinstatement of METH-seeking during adulthood in rats. The involvement of the oxytocinergic system in METH addiction is also supported by biochemical findings showing that systemic administration of OT decreases METH-induced enhancement in *Fos* expression in the subthalamic nucleus and AcbC in rats (see McGregor and Bowen, 2012) and that OTR binding is increased in the amygdala following a 10-day METH administration regimen in mice (Zanos et al., 2014b). Together, these findings provide evidence

for a key role of OT in METH addiction and highlight OT's "antireward/anticraving" and relapse prevention potential in METH addiction.

A possible mechanism underlying the effects of OT on METH addiction might involve its direct effects on the dopaminergic system in the brain. Indeed, it has been shown that systemic OT administration directly facilitates dopamine turnover in the striatum of treatment-naïve and cocaine-treated rats (see Sarnyai and Kovacs, 1994). Furthermore, Qi et al. (2008) demonstrated that i.c.v OT administration reduces METH-induced increase in dopamine turnover in the striatum of mice. Since METH use has been associated with lower levels of dopamine D_2 receptor (D_2R) availability in striatum (Wang et al., 2012), and OTR are co-localized and functionally interact with D_2R in striatum (Romero-Fernandez et al., 2013), it can be postulated that these two receptor systems might functionally interact to also regulate several METH addiction processes.

Numerous studies have also implicated the CRF system in METH addiction. CRF mRNA levels are increased in Acb following a single METH injection (Martin et al., 2012). Likewise, increased CRF levels were observed in the amygdala and plasma of rats undergoing withdrawal from METH self-administration (Nawata et al., 2012). Furthermore, administration of a non-selective CRF receptor antagonist attenuated stress-induced reinstatement of METH-seeking (Nawata et al., 2012) and administration of CRF-R_1 antagonists decreased both cue-and priming-induced reinstatement of *METH*-seeking (Moffett and Goeders, 2007). Interestingly, alterations in the CRF system have been shown to be associated with increased anxiety-like behavior and stress-induced reinstatement of METH-seeking in rodents (Nawata et al., 2012), indicating that the CRF system might be involved in the behavioral consequences of METH addiction, including anxiety and stress. CRF is considered as an important integrator of the hypothalamic-pituitary-adrenal (HPA) axis in the modulation of stress responses (Bale et al., 2002). METH administration has been also shown to induce a dysregulation of the hypothalamic-pituitary-adrenal (HPA) axis. Specifically, adolescent METH users have higher cortisol levels following

exposure to stress (King et al., 2010) and METH administration increases plasma corticosterone levels in rodents (Grace et al., 2010).

The MOPr system has been also shown to be involved in METH addiction processes. In particular, MOPr knockout mice exhibit decreased METH-induced hyper-locomotion and stereotypy and do not manifest behavioral sensitization to METH (Shen et al., 2010). Chiu et al. (2006) demonstrated a down-regulation of MOPr binding in brain membranes following an 8-day withdrawal period from chronic METH administration, which was followed by a rebound increase after 21 days of withdrawal in mice suggesting involvement of the MOPr system during METH abstinence. Conversely, MOPr gene expression and protein levels were reduced in the frontal cortex of mice following long-term withdrawal from repeated METH administration (Yamamoto et al., 2011).

Therefore, in the present study we aimed to characterize the behavioral consequences of METH abstinence in a mouse model of chronic METH use and withdrawal. Specifically, we hypothesized that withdrawal from chronic METH administration induces emotional impairment (i.e., anxiety and/or depression). We then investigated whether a 10-day METH administration and 7 days of withdrawal induce alterations on the central OT, D_2R, and MOPr systems, as well as on the HPA axis and the amygdalar CRF. This study assesses a whole range of different CNS systems in a mouse model of METH abstinence. Our findings shed light into brain region-specific neuroadaptations, which might be involved in driving specific METH abstinence-induced behaviors.

2. Materials and Methods

2.1 Animals

Male C57BL/6J mice (8-week old at the beginning of the experiments, Charles River, UK), were housed individually in a temperature-controlled environment with a 12-hour light/dark cycle (lights on: 06:00 am). Food and water were available *ad-libitum*. All experimental procedures were conducted in accordance with the U.K. Animal Scientific Procedures Act (1986).

2.2 Chronic steady-dose methamphetamine administration paradigm

Mice for all the experiments (see Figure 1 for experimental timelines) were randomly divided into four groups; saline-, METH-treated, saline-withdrawn and METH-withdrawn animals. Chronic METH-treated animals were injected i.p. for 10 days with METH (2 mg/kg) (Sigma-Aldrich, UK), once per day (09:00), in accordance with Zanos et al., (2014b). The chronic saline-treated group was administered with saline (10 ml/kg, i.p.) for 10 days, once per day (09:00). Saline-withdrawn and METH-withdrawn animals were treated with the same administration paradigm and left to spontaneously withdraw in their home-cages for a period of 7 days (unless otherwise stated), as previously described (Lu et al., 2010).

2.3 Behavioral characterization (experiment 1)

Mice were treated with chronic saline or a steady-dose METH administration paradigm (as described above) and then assessed for memory impairments (5 days withdrawal), anxiety- (7 days withdrawal) and depressive-like behaviors (8 days withdrawal) using the novel object recognition (NOR), elevated plus-maze (EPM) and forced-swim test (FST) respectively. These tests were performed in the same animals. The order of testing was determined by the degree of anxiety inducing properties of each test with the least stressful conducted first and the most potentially distressing test last (Clemens et al., 2007). The NOR and EPM were performed in dim lighting conditions (NOR 30 lux; EPM, 10 lux) and the FST was performed under normal lighting (300 lux).

Novel object recognition

The NOR was performed as previously described by Bevins and Besheer (2006) with minor modifications. Briefly, mice were habituated to the NOR arena (30cm x 20cm x 20cm; Linton Instrumentation, U.K.) for 20 minutes to reduce the novelty-induced stress. During the acquisition phase two identical objects (either dice or marbles stuck on a plastic square block) were placed in the arena and mice left to explore both objects for 20 minutes. The order of the objects was alternated between mice to avoid bias towards any of the objects. Following the acquisition phase mice were returned to their home cages for a retention time of 35 minutes. During the testing phase a familiar object and a novel object were placed in the arena and the mouse was re-introduced and left to explore for 2 minutes. All the three phases of the NOR (habituation, acquisition and testing) were performed on the same day. The sessions were recorded using a digital video-camera (Sony Handycam CX-250, Sony, Japan) and the time spent interacting (directly sniffing) with each object was scored by two observers blind to the treatment groups.

Elevated plus-maze

The elevated plus-maze was carried out as previously described in Zanos et al. (2014a). The time spent in the open and closed arms of the EPM during the 5-min test was measured by an automated tracking system (EthoVision v.3.0, Noldus Information Technology, Netherlands). Anxiety-like behavior was determined by calculating the amount of time spent and number of entries each mouse made in the open and closed arms and reported as the total time and the percentage number of entries in the open arms respectively.

Forced-swim test

The FST was carried out as previously described (Zanos et al., 2015a). Briefly, mice were placed individually into clear glass cylinders (25cm height x 17cm diameter) filled with 2.5 liters of water at room temperature (24±1^{o}C) for 6 minutes. The test session was recorded using a digital video-camera (Sony Handycam CX-250, Sony, Japan). Immobility time, defined as passive floating with no additional

activity other than that needed to keep the mouse head above water, was scored by two observers blind to the treatment groups for the last 4 minutes of the 6-min test. Latency to the first encounter of immobility was also measured. Fecal boli of the animals were counted at the end of the FST.

2.4 Locomotor and stereotypic activity measurements (experiment 2)

Locomotor activity of each mouse was measured daily (8:00 am) in locomotor chambers (40cm x 20cm x 20cm; Linton Instrumentation, U.K.) as previously described (Zanos et al. 2014a). During the administration period, mice were habituated in locomotor chambers for 60 minutes prior to saline/METH injections in order to assess basal activity. Then, mice received an i.p. injection of saline or METH (2 mg/kg) and were returned immediately to the locomotor chambers. Locomotor responses were measured immediately following the injection of the drugs. Horizontal and vertical (i.e., rearing) activities were measured for further 90 minutes. Locomotor responses of animals were monitored daily for the 10-day duration of the treatment and 7 days after the last treatment injection (withdrawal; day 17 – without any injections). Horizontal and vertical activities were recorded as the number of sequential infrared beam breaks, every 5 mins. The average activity, during both basal and stimulated activities, was calculated daily.

2.5 Biochemical and Neurochemical analysis (experiments 3-4)

Separate cohorts of male C57BL/6J mice were treated with an identical chronic saline and METH administration paradigm as described above, and some were left to spontaneously withdraw in their home cages for 7 days following their last treatment injection (4 treatment groups in total); where we observed the anxiety-like symptoms. Mice were euthanized by a 30-sec CO_2 exposure followed by decapitation 2.5 hours post-final injection for the chronic saline/METH administration groups or 7 days post-final injection for the withdrawal groups. For the withdrawal groups, mice were placed in the previously drug-associated locomotor chambers for a period of 1 hour prior to euthanasia.

2.5.1 Quantitative Receptor Autoradiography (experiment 3)

Coronal brain sections were cut (20 μm thick; 300 μm apart) using a cryostat (Zeiss Microm 505E, U.K.), thaw-mounted onto gelatin subbed ice-cold microscope slides and processed for autoradiography.

μ-opioid receptor binding. MOPr autoradiography was carried out in accordance with Georgiou et al., (2015a). For the determination of total binding, slides were incubated for 60 minutes in 4 nM [^{3}H]-tyrosyl-3,5-3H(N) (DAMGO) (PerkinElmer, 1905.5 GBq/mmol) in Tris-HCl (pH 7.4, room temperature). Adjacent sections were incubated in [^{3}H]DAMGO (4nM) in the presence of 1μM naloxone (Sigma-Aldrich, UK), to determine non-specific binding (NSB).

Oxytocin receptor binding. OTR autoradiography was carried out as previously described (Zanos et al., 2014a; Zanos et al., 2014b). For the determination of total binding, slides were incubated in 50pM [^{125}I]-ornithine vasotocin (OVTA) (PerkinElmer, 81.4 TBq/mmol) in an incubation buffer medium (50mM Tris–HCl, 10 mM $MgCl_2$, 1mM EDTA, 0.1% w/v bovine serum albumin, 0.05% w/v bacitracin; pH 7.4 at room temperature) for 60 minutes. For the determination of NSB, adjacent sections were incubated with [^{125}I]-OVTA (50pM) in the presence of 50μM unlabelled (Thr4, Gly7)-oxytocin (Bachem, Germany).

Dopamine D_2 receptor binding. Dopamine D_2R autoradiography was performed as detailed (Wright et al., 2015). For the determination of total binding, slides were incubated with 4nM [^{3}H]raclopride (PerkinElmer, Belgium) in Tris-HCl (pH 7.4, room temperature) for 90 minutes. For the determination of NSB, adjacent sections were incubated with [^{3}H]raclopride (4nM) in the presence of 10μM sulpiride (Tocris Biosciences, Bristol, UK).

Slides with brain sections from all the treatment groups were apposed on the same film (Kodak BioMax; Sigma-Aldrich, UK) along with appropriate ^{3}H and ^{14}C microscale standards (Amersham Pharmacia Biotech, U.K.) to allow quantification. Different apposition times were used depending on the autoradiographic binding (MOPr binding-10 weeks; OTR binding-3 days; D_2R binding–5 weeks).

2.5.2 Plasma corticosterone levels (experiment 3)

Trunk blood from saline- and METH-treated/withdrawn mice was collected in EDTA-containing tubes and spun for 15 min at 2000 x g at 4°C. Plasma was collected and corticosterone levels were measured using a rat/mouse corticosterone [^{125}I] kit (MP Biomedicals, USA), according to the manufacturer's instructions; also see Georgiou et al. (2015b).

2.5.3 Immunohistochemical measurement of CRF$^+$ neurons, c-Fos neuronal activity marker and c-Fos$^+$/CRF$^+$ co-labelled neurons (experiment 3)

CRF$^+$, c-Fos and c-Fos$^+$/CRF$^+$ immunohistochemical analysis in brain sections (20 μm thick; bregma -1.82mm; amygdala) was carried out as previously described (Garcia-Carmona et al., 2013). Briefly, for the double-labelling process, following the blocking of the samples with H_2O_2 and with 0.3% normal goat serum (Vector Laboratories, USA), tissue sections were incubated overnight at room temperature with a rabbit anti-c-Fos antibody (Santa Cruz Biotechnology). This was followed by application of a biotinylated anti-rabbit IgG (Vector Laboratories). Antigens were visualized using an avidin–biotin immunoperoxidase protocol according to manufacturer's instructions (Vectastasin ABC Elite kit, Vector Laboratories). 3,3′-diaminobenzidine (DAB) nickel-intensification (Sigma, USA) was used as a chromogen for c-Fos (black color). Then, sections were rinsed with PBS and were processed for CRF measurement using a rabbit anti-CRF antibody and revealed with DAB (brown color).

CRF$^+$ and c-Fos immunostaining as well as c-Fos$^+$/CRF$^+$ co-labelled neurons in the amygdala were quantified bilaterally for each mouse, for all treatment groups by an observer blind to the treatment groups. The density of CRF$^+$, c-Fos$^+$ and cFos$^+$/CRF$^+$ immunoreactivities was determined using a computer assisted image analysis system (Qwin; Leica, Spain). A square field (195 μm side) was superimposed upon the captured image (×10 magnification) to use as a reference area.

2.5.4 Oxytocin peptide levels in the brain and plasma (experiment 4)

Brains from a separate cohort of chronic saline/METH and withdrawn mice, treated with identical administration regimen as described above, were collected and hypothalamus, amygdala and striatum (Acb + CPu) were dissected and immediately preserved in dry ice and stored in -80^{o}C. Peptides were extracted as previously described (Zanos et al., 2014a). Briefly, tissues were mixed with 1M acetic acid, heated to 95^{o}C for 10 min, homogenized and stored in -80^{o}C overnight. The following day, samples were thawed on ice and centrifuged at 9000 x g for 20 min (4 ^{o}C) and the supernatant was collected and lyophilized. In all the extracted samples, OT content was measured by radioimmunoassay using iodinated tracer as previously described (Landgraf, 1981).

For plasma oxytocin level measurements, trunk blood from mice was collected in tubes containing EDTA and aprotinin (500 KIU/ml of blood). The samples were centrifuged at 1600 x g for 15 min (4^{o}C) and supernatants stored in -80^{o}C. Extraction of the peptide from plasma was carried out according to Landgraf (1981). The eluent from the extraction process was collected and lyophilized. Oxytocin brain and plasma peptide levels were measured by Prof. Landgraf's laboratory (Max Planck Institute of Psychiatry, Munich, Germany) using iodinated tracer in accordance with Landgraf (1981) and is reported as % of control (chronic saline group)

2.6 Statistical analysis

All values are expressed as the mean ± SEM. All statistical analyses were performed using GraphPad *v6* (GraphPad software Inc., La Jolla, CA, USA). Differences in locomotor and stereotypic (rearing) activities were analyzed using repeated measures two-way ANOVA with factors 'treatment (saline/METH)' and 'time (days; repeated factor)'. For assessing the development of locomotor sensitization, one-way repeated measures ANOVA ('time' as the repeated factor) was performed specifically for METH-treated mice. Fecal boli production during the FST was analyzed with non-parametric Mann-Whitney *U*-test. For the analysis of the effects of METH withdrawal on memory,

anxiety- and depressive-like behavior, unpaired Student's unpaired *t*-tests was used. For analysis of the relative OT levels and OTR, MOPr and D_2R binding, two-way ANOVA was performed in each individual brain region and plasma for factors 'treatment (saline/METH)' and 'experimental phase (chronic/withdrawal)'. Corticosterone, CRF^+, c-Fos^+, and c-Fos^+/CRF^+ levels were analyzed using a two-way ANOVA for factors 'treatment (saline/METH)' and 'experimental phase (chronic/withdrawal)'. ANOVAs were followed by Holm-Šídák *post-hoc* test when significance was reached (i.e., $p<0.05$). All statistical analyses, as well as the number of animals per group for each experiment are provided in Table 1.

Table 1: Statistical Analyses

	Statistical test	Treatment effect		Experimental phase		Interaction effect	
Overall effects for Figure 2							
Novel object recognition (n=6)		*Factor 'treatment'*					
Discrimination ratio	unpaired *t*-test	*p>0.05*					
Elevated plus-maze (n=6)		*Factor 'treatment'*					
Open-arm time	unpaired *t*-test	*p>0.05*					
% open-arm entries	unpaired *t*-test	*p<0.05**					
Forced-swim test (n=6)		*Factor 'treatment'*					
Immobility time	unpaired *t*-test	*p>0.05*					
Latency to first immobility	unpaired *t*-test	*p>0.05*					
Fecal boli	Mann Whitney *U*-test	*p<0.05**					
Overall effects for Figure 3							
METH effects on locomotor activity (n=13)		*Factor 'treatment'*		Factor 'time (days)'		*Factor 'treatment' x 'time'*	
Stimulated horizontal activity	two-way RM ANOVA	$F_{[1,24]}$=492.80;	*p<0.001**	$F_{[9,216]}$=1.35	*p=0.32*	$F_{[9,216]}$ = 3.48	*p<0.001**
Stimulated vertical activity	two-way RM ANOVA	$F_{[1,24]}$=16.10;	*p<0.001**	$F_{[9,216]}$=3.44	*p<0.001**	$F_{[9,216]}$ = 0.34	*p>0.05*
Basal horizontal activity (Days 1-10)	two-way RM ANOVA	$F_{[1,24]}$= 9.66	*p<0.01**	$F_{[9,216]}$= 31.83	*p<0.001**	$F_{[9,216]}$=3.16	*p<0.01**
Basal horizontal activity (Day 17)	unpaired *t*-test		*p<0.05**				
Basal vertical activity (Days 1-10)	two-way RM ANOVA	$F_{[1,24]}$= 15.56	*p<0.001**	$F_{[9,216]}$= 11.34	*p<0.001**	$F_{[9,216]}$=2.16	*p<0.05**
Basal vertical activity (Day 17)	unpaired *t*-test		*p<0.05**				
Overall effects for Figure 4							
OTR autoradiography (n=5-6)		*Factor 'treatment'*		Factor 'experimental phase'		*Factor 'treatment' x 'experimental phase'*	
AOM	two-way ANOVA	$F_{[1,20]}$=1.21	*p=0.28*	$F_{[1,20]}$=1.12	*p=0.30*	$F_{[1,20]}$=0.03	*p=0.87*
AOV	two-way ANOVA	$F_{[1,19]}$=0.23	*p=0.64*	$F_{[1,19]}$=1.067	*p=0.31*	$F_{[1,19]}$=1.71	*P=0.21*
AOL	two-way ANOVA	$F_{[1,19]}$=1.55	*p=0.23*	$F_{[1,19]}$=0.78	*p=0.39*	$F_{[1,19]}$=0.77	*p=0.39*
CgCx	two-way ANOVA	$F_{[1,19]}$=0.51	*p=0.48*	$F_{[1,19]}$=0.19	*p=0.67*	$F_{[1,19]}$=0.90	*p=0.36*
Pir	two-way ANOVA	$F_{[1,20]}$=1.64	*p=0.21*	$F_{[1,20]}$=2.39	*p=0.14*	$F_{[1,20]}$=0.65	*p=0.43*
AcbC	two-way ANOVA	$F_{[1,19]}$=0.24	*p=0.63*	$F_{[1,19]}$=0.001	*p=0.98*	$F_{[1,19]}$=0.07	*p=0.80*
AcbSh	two-way ANOVA	$F_{[1,19]}$=0.07	*p=0.79*	$F_{[1,19]}$=0.54	*p=0.47*	$F_{[1,19]}$=0.67	*p=0.43*
CPu	two-way ANOVA	$F_{[1,19]}$=0.46	*p=0.51*	$F_{[1,19]}$=0.03	*p=0.86*	$F_{[1,19]}$=1.00	*p=0.33*
MS	two-way ANOVA	$F_{[1,19]}$=0.58	*p=0.46*	$F_{[1,19]}$=0.0007	*p=0.98*	$F_{[1,19]}$=1.50	*p=0.24*
VDB	two-way ANOVA	$F_{[1,18]}$=1.17	*p=0.29*	$F_{[1,18]}$=0.49	*p=0.49*	$F_{[1,18]}$=3.35	*p=0.08*
LS	two-way ANOVA	$F_{[1,20]}$=8.61	*p<0.01**	$F_{[1,20]}$=7.35	*p<0.05**	$F_{[1,20]}$=7.00	*p<0.05**
Hip	two-way ANOVA	$F_{[1,19]}$=5.03	*p<0.05**	$F_{[1,19]}$=1.12	*p=0.30*	$F_{[1,19]}$=1.46	*p=0.24*
Th	two-way ANOVA	$F_{[1,19]}$=2.73	*p=0.12*	$F_{[1,19]}$=2.97	*p=0.10*	$F_{[1,19]}$=0.26	*p=0.62*
Hyp	two-way ANOVA	$F_{[1,19]}$=0.00002	*p=0.99*	$F_{[1,19]}$=0.17	*p=0.68*	$F_{[1,19]}$=1.19	*p=0.16*
Amy	two-way ANOVA	$F_{[1,19]}$=0.13	*p=0.76*	$F_{[1,19]}$=0.90	*p=0.36*	$F_{[1,19]}$=8.94	*p<0.01**
OT levels (n=6-7)		*Factor 'treatment'*		*Factor 'experimental phase'*		*Factor 'treatment' x 'experimental phase'*	
Striatum	two-way ANOVA	$F_{[1,23]}$=0.02	*p=0.88*	$F_{[1,23]}$=0.06	*p=0.81*	$F_{[1,23]}$=0.06	*p=0.81*
Hyp	two-way ANOVA	$F_{[1,23]}$=0.03	*p=0.85*	$F_{[1,23]}$=2.38	*p=0.14*	$F_{[1,23]}$=2.38	*p=0.14*
Amy	two-way ANOVA	$F_{[1,23]}$=0.27	*p=0.61*	$F_{[1,23]}$=3.46	*p=0.08*	$F_{[1,23]}$=3.46	*p=0.08*
Plasma	two-way ANOVA	$F_{[1,23]}$=1.99	*p=0.17*	$F_{[1,23]}$=3.77	*p=0.06*	$F_{[1,23]}$=3.77	*p=0.06*
Plasma corticosterone levels (n=5-6)		*Factor 'treatment'*		*Factor 'experimental phase'*		*Factor 'treatment' x 'experimental phase'*	
	two-way ANOVA	$F_{[1,19]}$=5.20	*p<0.05**	$F_{[1,19]}$=11.35	*p<0.01**	$F_{[1,19]}$=6.60	*p<0.05**
Overall effects for Figure 5							
MOPr autoradiography (n=5-6)		*Factor 'treatment'*		*Factor 'experimental phase'*		*Factor 'treatment' x 'experimental phase'*	
MtCx	two-way ANOVA	$F_{[1,18]}$=0.91	*p=0.35*	$F_{[1,18]}$=0.82	*p=0.38*	$F_{[1,18]}$=1.47	*p=0.24*
CgCx	two-way ANOVA	$F_{[1,19]}$=1.95	*p=0.18*	$F_{[1,19]}$=0.17	*p=0.69*	$F_{[1,19]}$=1.43	*p=0.25*
Pir	two-way ANOVA	$F_{[1,19]}$=1.04	*p=0.32*	$F_{[1,19]}$=3.17	*p=0.09*	$F_{[1,19]}$=0.17	*p=0.68*
AcbC	two-way ANOVA	$F_{[1,20]}$=16.96	*p<0.001**	$F_{[1,20]}$=0.02	*p=0.90*	$F_{[1,20]}$=1.02	*p=0.33*
AcbSh	two-way ANOVA	$F_{[1,20]}$=15.55	*p<0.001**	$F_{[1,20]}$=0.0005	*p=0.98*	$F_{[1,20]}$=0.62	*p=0.44*
CPu	two-way ANOVA	$F_{[1,20]}$=6.05	*p<0.05**	$F_{[1,20]}$=0.04	*p=0.84*	$F_{[1,20]}$=0.07	*p=0.79*
MS	two-way ANOVA	$F_{[1,19]}$=2.46	*p=0.13*	$F_{[1,19]}$=1.79	*p=0.20*	$F_{[1,19]}$=0.01	*p=0.92*
VDB	two-way ANOVA	$F_{[1,19]}$=1.76	*p=0.20*	$F_{[1,19]}$=2.75	*p=0.11*	$F_{[1,19]}$=0.82	*p=0.38*
LS	two-way ANOVA	$F_{[1,19]}$=0.34	*p=0.56*	$F_{[1,19]}$=1.29	*p=0.27*	$F_{[1,19]}$=0.001	*p=0.98*
Th	two-way ANOVA	$F_{[1,19]}$=0.41	*p=0.53*	$F_{[1,19]}$=0.25	*p=0.62*	$F_{[1,19]}$=0.10	*p=0.75*
Hyp	two-way ANOVA	$F_{[1,19]}$=0.04	*p=0.84*	$F_{[1,19]}$=0.31	*p=0.59*	$F_{[1,19]}$=0.0001	*p=0.99*
Hip	two-way ANOVA	$F_{[1,19]}$=0.17	*p=0.69*	$F_{[1,19]}$=0.17	*p=0.68*	$F_{[1,19]}$=0.07	*p=0.79*
Amy	two-way ANOVA	$F_{[1,19]}$=0.06	*p=0.81*	$F_{[1,19]}$=0.09	*p=0.77*	$F_{[1,19]}$=2.78	*p=0.11*
D_2 autoradiography (n=5-6)		*Factor 'treatment'*		*Factor 'experimental phase'*		*Factor 'treatment' x 'experimental phase'*	
AcbC	two-way ANOVA	$F_{[1,19]}$=1.11	*p=0.31*	$F_{[1,19]}$=1.01	*p=0.33*	$F_{[1,19]}$=0.02	*p=0.90*
AcbSh	two-way ANOVA	$F_{[1,19]}$=0.71	*p=0.41*	$F_{[1,19]}$=0.26	*p=0.62*	$F_{[1,19]}$=0.05	*p=0.83*
CPu	two-way ANOVA	$F_{[1,19]}$=0.57	*p=0.46*	$F_{[1,19]}$=0.97	*p=0.34*	$F_{[1,19]}$=0.02	*p=0.90*
Overall effects for Figure 6							
Amygdalar CRF levels (n=6)		*Factor 'treatment'*		*Factor 'experimental phase'*		*Factor 'treatment' x 'experimental phase'*	
CRF^+	two-way ANOVA	$F_{[1,20]}$=40.27	*p<0.001**	$F_{[1,20]}$=12.01	*p<0.01**	$F_{[1,20]}$=7.80	*p<0.05**
c-Fos^+	two-way ANOVA	$F_{[1,20]}$=2.39	*p=0.14*	$F_{[1,20]}$=0.001	*p=0.97*	$F_{[1,20]}$=0.47	*p=0.50*
c-Fos^+/CRF^+	two-way ANOVA	$F_{[1,20]}$=23.15	*p<0.001**	$F_{[1,20]}$=6.79	*p<0.05**	$F_{[1,20]}$=2.06	*p=0.18*

3. Results

3.1 Effects of METH withdrawal on memory, anxiety- and depressive-like behavior in mice

Novel object recognition. Memory performance was assessed using the NOR test following a 5-day abstinence from chronic METH treatment. METH-withdrawn animals did not manifest object recognition impairment, since there was no significant difference in the NOR discrimination ratio compared to saline controls (Figure 2A). No difference was observed in the distanced travelled (mm) during the habituation phase between the saline and METH withdrawal animals (Saline withdrawal: 3255 ± 188.2 *vs* METH withdrawal: 3060 ± 154.8).

Elevated plus-maze. Anxiety-related behavior in saline- and METH-withdrawn mice was assessed with the use of the EPM following the 7-day METH withdrawal period. Although, time spent in the open arms was not significantly different between METH-withdrawn and saline-withdrawn animals (Figure 2B), a significant decrease in the percentage of entries in the open arms of METH-withdrawn mice compared to saline-withdrawn controls was observed (Figure 2C), indicating an anxiogenic-like phenotype. There was no difference in total arm entries between saline and METH withdrawal groups (239.7±6.67 *vs* 241.0±5.25 respectively)

Forced-swim test. Depressive-like behavior in saline- and METH-withdrawn mice was assessed with the use of the FST following 8-day withdrawal from chronic METH administration. METH-withdrawn animals did not have any differences in their immobility time (Figure 2D) or latency to the first immobility count compared to saline-withdrawn animals (Figure 2E). However, METH-withdrawn mice produced significantly more fecal boli during the FST compared to saline-withdrawn mice (Figure 2F), indicative of increased anxiety-related emotionality (Craft et al., 2010; Marti and Armario, 1993).

3.2 Effects of chronic METH administration and withdrawal on basal and stimulated locomotor and stereotypic rearing activity in mice

METH pre-treatment significantly increased basal (non-injected) horizontal activity on Days 2-4; this effect did not persist throughout the 10-day METH administration paradigm (Figure 3A). Following the 7-day withdrawal period (day 17; no injections), animals that were receiving METH during the chronic phase showed an increase in their horizontal activity compared to their respective saline controls (Figure 3A). Horizontal locomotor activity on Day 17 was less than shown in Day 1 for the saline-treated mice ($p<0.001$; Day 17 *vs* Day 1), but not for the METH-treated mice ($p=0.1$; Day 17 *vs* Day 1), further suggesting a contextual- and possibly neuroplasticity-related METH-induced conditioned sensitization, without the presence of the drug (Figure 3A).

Horizontal stimulated activity of mice was increased following METH treatment throughout the 10-day administration paradigm compared with saline-treated mice (Figure 3B). From the second day of the administration paradigm, there was a significant increase in METH-stimulated horizontal activity which persisted until the end of the administration paradigm (i.e., Days 2-10) compared to Day 1~~, indicating the acquisition of behavioral sensitization to the acute locomotor-stimulating effect of MAP~~ (Figure 3B).

Pre-treatment with METH increased basal (non-injected) vertical activity from day 2 of the administration paradigm and was statistically significant on days 3,4,5,6,8 and 9 of METH administration compared to the saline controls (Figure 3C). Following the 7-day withdrawal period (day 17; no injections), animals receiving METH during the chronic phase showed an increase in their vertical activity compared to their respective saline controls (Figure 3C). Vertical (rearing) activity on Day 17 was less than Day 1 for control mice ($p<0.05$; Day 17 *vs* Day 1), but not for the METH-treated animals ($p=0.9$; Day 17 *vs* Day 1; Figure 3C).

Vertical stimulated activity was increased in METH-treated compared to saline-treated controls throughout the 10-day METH administration paradigm (Figure 3D).

3.3 Effect of METH administration and 7-day withdrawal on the OT system

Quantitative analysis of OTR binding showed a significant 'treatment' effect in the lateral septum (LS) and hippocampus (Figure 3A,B). An 'experimental phase' effect was also observed in LS. Moreover, a significant 'treatment' x 'experimental phase' interaction was identified in the LS and amygdala. LSD *post-hoc* test revealed a significant increase in OTR binding in the amygdala following the 10-day METH administration, which was normalized following the 7-day withdrawal period (Figure 4A,B). While chronic METH administration did not alter OTR binding in the LS, METH withdrawal induced a significant increase in OTR binding in that region (Figure 4A,B).

Chronic METH administration and withdrawal did not induce any alterations in the OT content in the striatum (Figure 4C), hypothalamus (Figure 4D) and amygdala (Figure 4E) compared to their respective controls. Chronic administration of METH increased plasma OT levels, which were normalized to control (saline withdrawal) levels following the 7-day METH withdrawal period (Figure 4F).

3.4 Effect of METH administration and 7-day withdrawal on the HPA-axis

A significant effect of 'treatment', 'experimental phase' and an interaction between 'treatment' x 'experimental phase' was observed in plasma corticosterone levels. Chronic METH treatment increased plasma corticosterone levels compared to saline controls (Figure 4G). However, corticosterone levels were comparable to the control group following a 7-day METH withdrawal period (Saline withdrawal *vs* METH withdrawal; Figure 4G).

3.5 Effect of the 10-day METH administration and 7-day withdrawal on MOPr binding in mice

Quantitative analysis of MOPr binding showed a significant 'treatment' effect in the nucleus accumbens core (AcbC), nucleus accumbens shell (AcbSh) and caudate putamen (CPu). No significant 'experimental phase' effect or 'treatment' x 'experimental phase' interaction was observed in any of the regions analyzed (Figure 5A,B).

3.6 Effect of the 10-day METH administration and 7-day withdrawal on dopamine D_2 receptor binding in mice

Quantitative analysis dopamine D_2R binding did not reveal any significant differences induced by METH administration or withdrawal in any of the regions analyzed (Figure 5C,D).

3.7 Effect of the 10-day METH administration and 7-day withdrawal on CRF levels in the amygdala in mice

Immunohistochemical analysis of CRF^+ neurons and c-Fos^+/CRF^+ neurons in the amygdala showed a significant 'treatment' and 'experimental phase' effect following METH administration and withdrawal (Figure 6A-G). Two-way ANOVA revealed a significant 'treatment' x 'experimental phase' interaction in amygdalar CRF^+ neurons. Chronic METH treatment and withdrawal induced an increase in both amygdalar CRF^+ neurons (Figure 6A-D,E) and c-Fos^+/CRF^+ neurons in METH–treated animals compared to saline-treated animals, which persisted during withdrawal (Figure 6A-D,G). No significant difference was observed in the number of c-Fos^+ neurons between the METH- and saline-treated, as well as between the METH-withdrawn and saline-withdrawn animals (Figure 6A-D,F).

4. Discussion

In the present study we demonstrated that a 10-day METH administration induced a significant increase in OTR binding in the amygdala and caused an increase in the MOPr binding in the AcbC, AcbSh and CPu. These receptor changes were accompanied by an increase in plasma corticosterone and OT, as well as amygdalar CRF levels. Following a 7-day withdrawal period, while plasma corticosterone levels and amygdalar OTR binding returned to baseline levels, an up-regulation of OTR binding was observed in the LS. Increased striatal MOPr binding and amygdalar CRF levels persisted during METH withdrawal. These alterations during METH withdrawal were concomitant with an anxiogenic-like phenotype.

We firstly behaviorally characterized a mouse model of METH abstinence from chronic steady-dose METH administration regimen. Although METH withdrawal did not induce memory impairments, or depressive-like behaviors in our mouse model, anxiety-like symptoms were observed, including decreased open-arm entries in the EPM and increased defecation during the FST session, which has been previously associated with measures of anxiety (Walf and Frye, 2007) and emotionality (Craft et al., 2010; Marti and Armario, 1993) respectively. These findings are in line with previous studies showing anxiety-like symptoms following withdrawal from METH self-administration (Nawata et al., 2012) and following a steady-dose injection regimen of METH (Kitanaka et al., 2010) in rodents, and anxiety traits in METH-abstinent individuals (London et al., 2004), highlighting the translational value of our model and a direct link between METH abstinence and the emergence of a negative emotional state. Interestingly, anxiety symptoms were observed in METH users during the first two weeks of abstinence; a period considered being critical for relapse to METH administration (Mancino et al., 2011). Therefore, it has been postulated that the observed anxiety-related symptoms during withdrawal might act as a motivational trigger to re-administer the drug and relapse (Zorick et al., 2010). These anxiety-related symptoms were not associated with memory deficits as assessed by the novel object recognition task in our study.

Similar to a previous study demonstrating early withdrawal (i.e., 2 days withdrawal) but not protracted withdrawal (i.e., 15 days withdrawal) depressive-like symptoms in rats (Jang et al., 2013), we did not observe a depressive-like phenotype in the forced-swim test in METH-withdrawn mice. In agreement, Zorick et al. (2010) demonstrated that depressive symptoms resolved within a week of abstinence in METH-dependent humans. Administration of methamphetamine induced environment-specific increase in basal locomotor activity of mice, indicative of a conditioned/contextual sensitization to the drug-paired environment in anticipation for the METH injection. While METH-treated mice did not show contextual sensitization following 4 days of treatment, plausibly due to learning-related habituation to the drug-associated environment, they express higher locomotor activity in the previously METH-paired environment even 7 days following withdrawal, at a time point which METH (2 mg/kg) has been shown to be undetectable in both the brain and plasma of mice (Zombeck et al., 2009). Increased locomotor activity in the previously drug-paired environment has been linked with contextual sensitization (Robinson et al., 1998) and these long-lasting behavioral changes have been associated with persistent molecular neuroadaptations/neuronal plasticity (Ron and Jurd, 2005). Such long-term brain neuroadaptations have been hypothesized to contribute to drug craving following abstinence (Robinson and Berridge, 2008; Ron and Jurd, 2005; Sato, 1992; Sato et al., 1983). Interestingly, we have not only observed increased horizontal locomotor activity in the previously drug-paired compartment following withdrawal, but also increased stereotyped-movement (rearing behavior). Notably, memory impairment is unlikely to underlie these locomotor changes, since we show intact memory performance in the NOR task during METH abstinence. Increased psychostimulant-induced repetitive stereotypic/rearing behavior has been previously associated with psychotic properties of drugs of abuse (Reeves et al., 2003) and general psychotic symptoms in animals (see Forrest et al., 2014). Additionally, disruptions of pre-pulse inhibition were reported in mice following a similar administration/withdrawal paradigm used in the present study (7-day METH (1 mg/kg) administration and 7-day withdrawal; (Arai et al., 2008)). Taken together, increased baseline stereotypic/rearing behavior following the 7-day abstinence period observed in the present study might be possibly related to the prolonged psychotomimetic properties of METH.

Additionally, increased rearing activity has been also shown to reflect increased anxiety-like behaviors in mice (Lever et al., 2006), which indeed might be the case here too, since it is in line with the behavioral changes observed in the elevated plus-maze.

Evidence has implicated MOPr in the regulation of psychostimulant-induced behavioral sensitization. In particular, Shen et al., (2010) has demonstrated that MOPr knockout mice do not develop METH-induced locomotor sensitization and MOPr binding was shown to be increased in mouse brain tissue membranes 14 days following withdrawal from a METH sensitization protocol (Chiu et al., 2006), suggesting a clear involvement of MOPr in METH-induced sensitization. In the present study we demonstrated increased MOPr binding in the Acb and CPu following METH administration and withdrawal, which might be associated with the observed behavioral sensitization to the METH-associated environment during abstinence. Although it is not clear whether this receptor upregulation is associated with increased relapse potential following abstinence, the fact that Gorelick et al. (2008) have shown a positive correlation between MOPr binding in frontal and temporal cortices with relapse potential of cocaine use in former cocaine addicts along with our results point towards the need for further investigation for a possible role of the MOPr system in the modulation of psychostimulant craving during abstinence.

Chronic methamphetamine administration induced an upregulation of the OTR binding specifically in the amygdala and hippocampus, suggesting region-specific neuroadaptations of the oxytocinergic system following chronic methamphetamine treatment. An increase in amygdalar OTR binding was previously observed following chronic administration of other drugs of abuse, including cocaine (Georgiou et al., 2015a), morphine (Zanos et al., 2014a) and nicotine (Zanos et al., 2015b), highlighting a possible common mechanism of multiple drugs of abuse on the oxytocinergic system, which might be involved in several behavioral consequences of chronic drug use. However, in the present study amygdalar OTR binding returned to control levels following the 7-day withdrawal period, suggesting that this brain region specific neuroadaptation of the oxytocinergic system is not persistent after discontinuation of drug

administration and thus, unlikely to be involved in the methamphetamine withdrawal-induced anxiogenic phenotype. Similarly, chronic METH administration induced an upregulation of plasma oxytocin levels, which returned to control levels following 7 days of withdrawal. While the effects of acute METH administration on the central OTR system and plasma oxytocin levels are yet to be determined, it is unlikely that the observed upregulation of amygdalar OTR and plasma OT levels ~~to~~ reflect the acute effects of the drug since Sarnyai et al., 1992 has previously reported no effects of acute cocaine (another psychostimulant drug) on oxytocin content in plasma and amygdala. In support, acute doses of methamphetamine did not alter plasma OT levels in healthy adults (Bershad et al., 2015). In contrast to the normalized levels of plasma OT and amygdalar OTR binding following methamphetamine abstinence, we observed an increase in hippocampal OTR binding, which persisted following withdrawal (treatment effect). Interestingly, dysregulation of the hippocampal OT system has been also reported following chronic administration of cocaine (Sarnyai et al., 1992).

Importantly, METH withdrawal, but not chronic METH administration, triggered an increase in OTR binding in the LS, a region known to be involved in emotionality (see Sheehan et al., 2004). Interestingly, an increase in OTR in LS was also observed following a 7-day morphine withdrawal in mice and this was shown to be associated with withdrawal-induced anxiety (Zanos et al., 2014a). Considering that the septum is a brain region hypothesized to be responsible for the anxiolytic effects of OT (Lukas et al., 2013), it is likely that the dysregulation of the OTR system in the LS to be a possible mechanism underlying the anxiety-related symptoms observed in the present study. In fact, we have previously shown that decreased OT content in the brain was concomitant with an increase in the OTR in the lateral septum (Zanos et al., 2014). In addition, Zoicas et al., (2014) have demonstrated that social fear conditioning was associated with an increase in OTR binding in the septum of rodents, whereas i.c.v. administration of OT prevented social fear conditioning, suggesting a possible decreased local OT neurotransmission in that brain region to account for the increased OTR binding. However, further studies

investigating the effects of intra-LS administration of OT are needed to shed light in the exact role of this OT system dysregulation and its correlation with the METH abstinence-induced anxiety.

Anxiety-related behaviors have also been extensively linked with changes in both the HPA axis activity (see Faravelli et al., 2012), as well as hyper-activation of the CRF system in the brain in rodents (see Zorrilla et al., 2014). Here, an increase in plasma corticosterone levels was observed following chronic METH treatment, which was normalized after withdrawal. These findings suggest that METH withdrawal-induced anxiety-like symptoms are likely not associated with a dysregulation of the peripheral arm of the HPA-axis. In contrast, a persistent increase in amygdalar CRF^+ and c-Fos^+/CRF^+ neurons was demonstrated following the 10-day METH administration, and this effect was even enhanced during withdrawal, highlighting an important role of persistent neuroadaptations in the amygdalar CRF system to underlie behavioral changes occurring during METH abstinence. Interestingly, it has been previously suggested that increase activity of the CRF system in the amygdala is associated with drug abstinence-induced anxiety (see Zorrilla et al., 2014), suggesting a possible involvement of the increased amygdalar CRF levels in the development of anxiety-like behaviors in METH-withdrawn animals. However, more work needs to be carried out to verify the role of increased CRF in drug–withdrawal induced anxiety.

While we have previously shown that chronic administration of METH does not change D_2R binding in mice (Wright et al., 2015), in the present study we observed no alterations of the D_2R binding following 7 days of withdrawal, possibly suggesting that alterations in the D_2R are not involved in the observed anxiogenic phenotype. However, neuroadaptations on the D_2R system occurring downstream the receptor level cannot be precluded.

Conclusions: Overall, this study demonstrated alterations on the OTR, MOPr and CRF systems following chronic METH administration and withdrawal in brain regions functionally associated with the observed anxiety-related symptoms during abstinence. Our findings provide further insight into the specific neurobiological mechanisms underlying METH use and abstinence and provide information for potential

targets for the development of novel and effective pharmacotherapies for the treatment of METH addiction and prevention of relapse and comorbid anxiety.

5. Role of funding sources

Funding for this study was provided by a Royal Society grant (RG120556; P.I. Alexis Bailey) and by Lilia and Charalambos Georgiou. JAGC was in receipt of a pre-doctoral fellowship from Fundación Séneca, Agencia de Ciencia y Tecnología de la Región de Murcia (15519/FPI/10). The sponsors had no involvement in the design of the study and in the collection, analyses and interpretation of the data, nor in the writing of the manuscript and the decision to submit this article for publication.

6. Conflict of interest

The authors declare no conflict of interest.

7. References

Arai, S., Takuma, K., Mizoguchi, H., Ibi, D., Nagai, T., Takahashi, K., Kamei, H., Nabeshima, T., Yamada, K., 2008. Involvement of pallidotegmental neurons in methamphetamine- and MK-801-induced impairment of prepulse inhibition of the acoustic startle reflex in mice: reversal by GABAB receptor agonist baclofen. Neuropsychopharmacology 33, 3164-3175.

Bale, T.L., Lee, K.F., Vale, W.W., 2002. The role of corticotropin-releasing factor receptors in stress and anxiety. Integr Comp Biol 42, 552-555.

Baracz, S.J., Everett, N.A., McGregor, I.S., Cornish, J.L., 2014. Oxytocin in the nucleus accumbens core reduces reinstatement of methamphetamine-seeking behaviour in rats. Addict Biol. doi: 10.1111/adb.12198.

Bershad, A.K., Kirkpatrick, M.G., Seiden, J.A., de Wit H., 2015. Effects of acute doses of prosocial drugs methamphetamine and alcohol on plasma oxytocin levels. J Clin Psychopharmacol 35, 308-312.

Bevins, R.A., Besheer, J., 2006. Object recognition in rats and mice: a one-trial non-matching-to-sample learning task to study 'recognition memory'. Nat Protoc 1, 1306-1311.

Carson, D.S., Cornish, J.L., Guastella, A.J., Hunt, G.E., McGregor, I.S., 2010. Oxytocin decreases methamphetamine self-administration, methamphetamine hyperactivity, and relapse to methamphetamine-seeking behaviour in rats. Neuropharmacology 58, 38-43.

Chiu, C.T., Ma, T., Ho, I.K., 2006. Methamphetamine-induced behavioral sensitization in mice: alterations in mu-opioid receptor. J Biomed Sci 13, 797-811.

Clemens, K.J., Cornish, J.L., Hunt, G.E., McGregor, I.S., 2007. Repeated weekly exposure to MDMA, methamphetamine or their combination: long-term behavioural and neurochemical effects in rats. Drug Alcohol Depend 86, 183-190.

Cox, B.M., Young, A.B., See, R.E., Reichel, C.M., 2013. Sex differences in methamphetamine seeking in rats: impact of oxytocin. Psychoneuroendocrinology 38, 2343-2353.

Craft, R.M., Kostick, M.L., Rogers, J.A., White, C.L., Tsutsui, K.T., 2010. Forced swim test behavior in postpartum rats. Pharmacol Biochem Behav 96, 402-412.

Eslami-Shahrbabaki, M., Fekrat, A., Mazhari, S., 2015. A Study of the Prevalence of Psychiatric Disorders in Patients with Methamphetamine-Induced Psychosis. Addict Health 7, 37-46.

Faravelli, C., Lo Sauro, C., Lelli, L., Pietrini, F., Lazzeretti, L., Godini, L., Benni, L., Fioravanti, G., Talamba, G.A., Castellini, G., Ricca, V., 2012. The role of life events and HPA axis in anxiety disorders: a review. Curr Pharm Des 18, 5663-5674.

Forrest, A. D., Coto, C. A., Siegel, S. J., 2014. Animal Models of Psychosis: Current State and Future Directions. Current behavioral neuroscience reports 1, 100-116.

Garcia-Carmona, J.A., Milanes, M.V., Laorden, M.L., 2013. Brain stress system response after morphine-conditioned place preference. Int J Neuropsychopharmacol 16, 1999-2011.

Georgiou, P., Zanos, P., Ehteramyan, M., Hourani, S., Kitchen, I., Maldonado, R., Bailey, A., 2015a. Differential regulation of mGlu5R and MOPr by priming- and cue-induced reinstatement of cocaine-seeking behaviour in mice. Addict Biol. 20, 902-912.

Georgiou, P., Zanos, P., Garcia-Carmona, J. A., Hourani, S., Kitchen, I., Kieffer, B. L., Laorden, M. L., Bailey, A., 2015b. The oxytocin analogue carbetocin prevents priming-induced reinstatement of morphine-seeking: Involvement of dopaminergic, noradrenergic and MOPr systems. Eur Neuropsychopharmacol 25, 2459-2464.

Gorelick, D.A., Kim, Y.K., Bencherif, B., Boyd, S.J., Nelson, R., Copersino, M.L., Dannals, R.F., Frost, J.J., 2008. Brain mu-opioid receptor binding: relationship to relapse to cocaine use after monitored abstinence. Psychopharmacology (Berl) 200, 475-486.

Grace, C.E., Schaefer, T.L., Herring, N.R., Graham, D.L., Skelton, M.R., Gudelsky, G.A., Williams, M.T., Vorhees, C.V., 2010. Effect of a neurotoxic dose regimen of (+)-methamphetamine on behavior, plasma corticosterone, and brain monoamines in adult C57BL/6 mice. Neurotoxicol Teratol 32, 346-355.

Han, W.Y., Du, P., Fu, S.Y., Wang, F., Song, M., Wu, C.F., Yang, J.Y., 2014. Oxytocin via its receptor affects restraint stress-induced methamphetamine CPP reinstatement in mice: Involvement of the medial prefrontal cortex and dorsal hippocampus glutamatergic system. Pharmacol Biochem Behav 119, 80-87.

Hicks, C., Cornish, J.L., Baracz, S.J., Suraev, A., McGregor, I.S., 2014. Adolescent pre-treatment with oxytocin protects against adult methamphetamine-seeking behavior in female rats. Addict Biol. doi: 10.1111/adb.12197.

Jang, C.G., Whitfield, T., Schulteis, G., Koob, G.F., Wee, S., 2013. A dysphoric-like state during early withdrawal from extended access to methamphetamine self-administration in rats. Psychopharmacology (Berl) 225, 753-763.

King, G., Alicata, D., Cloak, C., Chang, L., 2010. Psychiatric symptoms and HPA axis function in adolescent methamphetamine users. J Neuroimmune Pharmacol 5, 582-591.

Kitanaka, N., Kitanaka, J., Tatsuta, T., Tanaka, K., Watabe, K., Nishiyama, N., Morita, Y., Takemura, M., 2010. Withdrawal from fixed-dose injection of methamphetamine decreases cerebral levels of 3-methoxy-4-hydroxyphenylglycol and induces the expression of anxiety-related behavior in mice. Neurochem Res 35, 749-760.

Landgraf, R., 1981. Simultaneous measurement of arginine vasopressin and oxytocin in plasma and neurohypophyses by radioimmunoassay. Endokrinologie 78, 191-204.

Lever, C., Burton, S., O'Keefe, J., 2006. Rearing on hind legs, environmental novelty, and the hippocampal formation. Rev Neurosci 17, 111-133.

London, E.D., Simon, S.L., Berman, S.M., Mandelkern, M.A., Lichtman, A.M., Bramen, J., Shinn, A.K., Miotto, K., Learn, J., Dong, Y., Matochik, J.A., Kurian, V., Newton, T., Woods, R., Rawson, R., Ling, W., 2004. Mood disturbances and regional cerebral metabolic abnormalities in recently abstinent methamphetamine abusers. Arch Gen Psychiatry 61, 73-84.

Lu, P., Mamiya, T., Lu, L., Mouri, A., Niwa, M., Kim, H.C., Zou, L.B., Nagai, T., Yamada, K., Ikejima, T., Nabeshima, T., 2010. Silibinin attenuates cognitive deficits and decreases of dopamine and serotonin induced by repeated methamphetamine treatment. Behav Brain Res 207, 387-393.

Lukas, M., Toth, I., Veenema, A.H., Neumann, I.D., 2013. Oxytocin mediates rodent social memory within the lateral septum and the medial amygdala depending on the relevance of the social stimulus: male juvenile versus female adult conspecifics. Psychoneuroendocrinology 38, 916-926.

Mancino, M.J., Gentry, B.W., Feldman, Z., Mendelson, J., Oliveto, A., 2011. Characterizing methamphetamine withdrawal in recently abstinent methamphetamine users: a pilot field study. Am J Drug Alcohol Abuse 37, 131-136.

Marti, J., Armario, A., 1993. Effects of diazepam and desipramine in the forced swimming test: influence of previous experience with the situation. Eur J Pharmacol 236, 295-299.

Martin, T.A., Jayanthi, S., McCoy, M.T., Brannock, C., Ladenheim, B., Garrett, T., Lehrmann, E., Becker, K.G., Cadet, J.L., 2012. Methamphetamine causes differential alterations in gene expression and patterns of histone acetylation/hypoacetylation in the rat nucleus accumbens. PLoS One 7, e34236.

McGregor, I.S., Bowen, M.T., 2012. Breaking the loop: oxytocin as a potential treatment for drug addiction. Horm Behav 61, 331-339.

Moffett, M.C., Goeders, N.E., 2007. CP-154,526, a CRF type-1 receptor antagonist, attenuates the cue- and methamphetamine-induced reinstatement of extinguished methamphetamine-seeking behavior in rats. Psychopharmacology (Berl) 190, 171-180.

Nawata, Y., Kitaichi, K., Yamamoto, T., 2012. Increases of CRF in the amygdala are responsible for reinstatement of methamphetamine-seeking behavior induced by footshock. Pharmacol Biochem Behav 101, 297-302.

Panenka, W.J., Procyshyn, R.M., Lecomte, T., MacEwan, G.W., Flynn, S.W., Honer, W.G., Barr, A.M., 2013. Methamphetamine use: a comprehensive review of molecular, preclinical and clinical findings. Drug Alcohol Depend 129, 167-179.

Qi, J., Yang, J.Y., Song, M., Li, Y., Wang, F., Wu, C.F., 2008. Inhibition by oxytocin of methamphetamine-induced hyperactivity related to dopamine turnover in the mesolimbic region in mice. Naunyn Schmiedebergs Arch Pharmacol 376, 441-448.

Qi, J., Yang, J.Y., Wang, F., Zhao, Y.N., Song, M., Wu, C.F., 2009. Effects of oxytocin on methamphetamine-induced conditioned place preference and the possible role of glutamatergic

neurotransmission in the medial prefrontal cortex of mice in reinstatement. Neuropharmacology 56, 856-865.

Reeves, R., Thiruchelvam, M., Richfield, E.K., Cory-Slechta, D.A., 2003. Behavioral sensitization and long-term neurochemical alterations associated with the fungicide triadimefon. Pharmacol Biochem Behav 76, 315-326.

Reichel, C.M., Schwendt, M., McGinty, J.F., Olive, M.F., See, R.E., 2011. Loss of object recognition memory produced by extended access to methamphetamine self-administration is reversed by positive allosteric modulation of metabotropic glutamate receptor 5. Neuropsychopharmacology 36, 782-792.

Robinson, T.E., Berridge, K.C., 2008. Review. The incentive sensitization theory of addiction: some current issues. Philos Trans R Soc Lond B Biol Sci 363, 3137-3146.

Robinson, T.E., Browman, K.E., Crombag, H.S., Badiani, A., 1998. Modulation of the induction or expression of psychostimulant sensitization by the circumstances surrounding drug administration. Neurosci Biobehav Rev 22, 347-354.

Romero-Fernandez, W., Borroto-Escuela, D.O., Agnati, L.F., Fuxe, K., 2013. Evidence for the existence of dopamine D2-oxytocin receptor heteromers in the ventral and dorsal striatum with facilitatory receptor-receptor interactions. Mol Psychiatry 18, 849-850.

Ron, D., Jurd, R., 2005. The "ups and downs" of signaling cascades in addiction. Sci STKE 2005, re14.

Sarnyai, Z., Kovacs, G.L., 1994. Role of oxytocin in the neuroadaptation to drugs of abuse. Psychoneuroendocrinology 19, 85-117.

Sarnyai, Z., Vecsernyes, M., Laczi, F., Biro, E., Szabo, G., Kovacs, G.L., 1992. Effects of cocaine on the contents of neurohypophyseal hormones in the plasma and in different brain structures in rats. Neuropeptides 23, 27-31.

Sato, M., 1992. A lasting vulnerability to psychosis in patients with previous methamphetamine psychosis. Ann N Y Acad Sci 654, 160-170.

Sato, M., Chen, C.C., Akiyama, K., Otsuki, S., 1983. Acute exacerbation of paranoid psychotic state after long-term abstinence in patients with previous methamphetamine psychosis. Biol Psychiatry 18, 429-440.

Sheehan, T.P., Chambers, R.A., Russell, D.S., 2004. Regulation of affect by the lateral septum: implications for neuropsychiatry. Brain Res Brain Res Rev 46, 71-117.

Shen, X., Purser, C., Tien, L.T., Chiu, C.T., Paul, I.A., Baker, R., Loh, H.H., Ho, I.K., Ma, T., 2010. mu-Opioid receptor knockout mice are insensitive to methamphetamine-induced behavioral sensitization. J Neurosci Res 88, 2294-2302.

Walf, A.A., Frye, C.A., 2007. The use of the elevated plus maze as an assay of anxiety-related behavior in rodents. Nat Protoc 2, 322-328.

Wang, G.J., Smith, L., Volkow, N.D., Telang, F., Logan, J., Tomasi, D., Wong, C.T., Hoffman, W., Jayne, M., Alia-Klein, N., Thanos, P., Fowler, J.S., 2012. Decreased dopamine activity predicts relapse in methamphetamine abusers. Mol Psychiatry 17, 918-925.

Wright, S.R., Zanos, P., Georgiou, P., Yoo, J.H., Ledent, C., Hourani, S.M., Kitchen, I., Winsky-Sommerer, R., Bailey, A., 2015. A critical role of striatal A R-mGlu R interactions in modulating the psychomotor and drug-seeking effects of methamphetamine. Addict Biol. doi: 10.1111/adb.12259.

Yamamoto, H., Takamatsu, Y., Imai, K., Kamegaya, E., Hagino, Y., Watanabe, M., Yamamoto, T., Sora, I., Koga, H., Ikeda, K., 2011. MOP Reduction During Long-Term Methamphetamine Withdrawal was Restored by Chronic Post-Treatment with Fluoxetine. Curr Neuropharmacol 9, 73-78.

Zanos, P., Georgiou, P., Wright, S.R., Hourani, S.M., Kitchen, I., Winsky-Sommerer, R., Bailey, A., 2014a. The oxytocin analogue carbetocin prevents emotional impairment and stress-induced reinstatement of opioid-seeking in morphine-abstinent mice. Neuropsychopharmacology 39, 855-865.

Zanos, P., Wright, S.R., Georgiou, P., Yoo, J.H., Ledent, C., Hourani, S.M., Kitchen, I., Winsky-Sommerer, R., Bailey, A., 2014b. Chronic methamphetamine treatment induces oxytocin receptor up-regulation in the amygdala and hypothalamus via an adenosine A2A receptor-independent mechanism. Pharmacol Biochem Behav 119, 72-79.

Zanos, P., Piantadosi, S.C., Wu, H.Q., Pribut, H.J., Dell, M.J., Can, A., Snodgrass, H.R., Zarate, C.A., Jr., Schwarcz, R., Gould, T.D., 2015a. The prodrug 4-chlorokynurenine pauses ketamine-like antidepressant effects, but not side effects, by NMDA/glycine$_B$-site inhibition. J Pharmacol Exp Ther 355, 76-85.

Zanos, P., Georgiou, P., Metaxas, A., Kitchen, I., Winsky-Sommerer, R., Bailey, A., 2015b. Region-specific up-regulation of oxytocin receptor binding in the brain of mice following chronic nicotine administration. Neurosci Lett. 600, 33-37.

Zoicas, I., Slattery, D. A., Neumann, I. D., 2014. Brain oxytocin in social fear conditioning and its extinction: involvement of the lateral septum. Neuropsychopharmacology 39, 3027-3035.

Zombeck, J.A., Gupta, T., Rhodes, J.S., 2009. Evaluation of a pharmacokinetic hypothesis for reduced locomotor stimulation from methamphetamine and cocaine in adolescent versus adult male C57BL/6J mice. Psychopharmacology (Berl) 201, 589-599.

Zorick, T., Nestor, L., Miotto, K., Sugar, C., Hellemann, G., Scanlon, G., Rawson, R., London, E.D., 2010. Withdrawal symptoms in abstinent methamphetamine-dependent subjects. Addiction 105, 1809-1818.

Zorrilla, E.P., Logrip, M.L., Koob, G.F., 2014. Corticotropin releasing factor: a key role in the neurobiology of addiction. Front Neuroendocrinol 35, 234-244.

8. Acknowledgments

The authors thank Prof. Rainer Landgraf for performing the tissue and blood oxytocin determinations. We also gratefully thank Dr. Helen Keyworth for her assistance in the statistical analyses.

9. Figure legends

Figure 1: Behavioral and tissue/plasma collection experimental timelines. Experimental timelines for the **(A)** behavioral characterization, **(B)** locomotor and stereotypic activity, **(C)** OTR, MOPr, D_2R, CRF and corticosterone, as well as **(D)** oxytocin content measurements. *Abbreviations:* CRF, corticotropin-releasing factor; D_2R, dopamine D_2 receptor; EPM, elevated plus-maze; FST, forced-swim test; METH, methamphetamine; MOPr, μ-opioid receptor; NOR, novel object recognition; OT, oxytocin; OTR, oxytocin receptor.

Figure 2: Anxiety-like behaviors and following 7 days methamphetamine withdrawal. Male C57BL/6J mice were treated with either saline or 10- day steady-dose methamphetamine (METH) administration paradigm (2 mg/kg, i.p. per day), followed by 5-8 days withdrawal. **(A)** Memory of the saline- and methamphetamine-withdrawn mice (5 days of withdrawal) was assessed in in the novel object recognition task. The discrimination ratio represents the time spent interacting with novel object/ total interaction time with both objects. **(B)** Open-arm time in the elevated plus-maze (EPM) (7 days of withdrawal) and **(C)** percentage open arm entries were measured to assess anxiety-like behaviors following 7 days of methamphetamine withdrawal. **(D)** Immobility time and **(E)** latency to first immobility count were assessed in the forced-swim test (FST) following 8 days methamphetamine withdrawal. **(F)** Fecal boli in the FST were counted as a measure of emotionality of methamphetamine- and saline-withdrawn mice. Data are expressed as the mean ± SEM. $*p<0.05$ (Student's unpaired *t*-test).

Figure 3: Effect of chronic METH administration and withdrawal on horizontal and vertical locomotor activity. Male C57BL/6J mice were treated with either saline or methamphetamine (METH) with a 10- day steady-dose administration paradigm (2 mg/kg, i.p. per day) and left to spontaneously withdrawal for 7 days. Average basal **(A)** horizontal and **(C)** vertical activities (representing stereotypic rearing) were measured daily in 5-min bins for 60 minutes pre-METH or saline injection during the 10-day steady-dose METH and saline administration paradigm (Days 1-10), as well as 7 days post-last injection (Day 17). Average stimulated **(B)** horizontal and **(D)** vertical activity were measured daily in 5-

min bins for 90 minutes post-METH or saline injection during the 10-day steady-dose METH and saline administration paradigm (Days 1-10). Data are expressed as mean ± SEM. *$p<0.05$, **$p<0.01$, ***$p<0.001$ vs saline; $^{\#\#}$ $p<0.01$; $^{\#\#\#}$ $p<0.001$ *vs* Day 1 (repeated measures two-way ANOVA followed by LSD *post-hoc* test).

Figure 4: Effect of chronic methamphetamine administration and withdrawal on [^{125}I]-OVTA binding to OTR, OT content and plasma corticosterone levels. Male C57BL/6J mice were treated either with saline or methamphetamine (METH) with a 10-day steady-dose administration paradigm (2 mg/kg, i.p. per day) and left to spontaneously withdraw for a period of 7 days. (**A)** Computer-enhanced representative OTR autoradiograms of adjacent coronal brain sections from chronic saline-, METH-treated, saline-withdrawn and METH-withdrawn mice at the level of the caudate putamen (Bregma 0.86mm, first row) and the thalamus (Bregma -2.06mm, second row). OTRs were labelled with [^{125}I]-OVTA (50pM). The color bar illustrates a pseudo-color interpretation of black and white film images in fmol/mg tissue equivalent. Representative images for the non-specific binding (50pM [^{125}I]-OVTA in the presence of 50μM unlabelled oxytocin) are shown for all the treatment groups. **(B)** Quantitative oxytocin receptor autoradiographic binding in brain regions of mice treated with a chronic 10-day steady-dose METH administration paradigm and in mice-withdrawn for 7 days. Oxytocin levels in **(C)** striatum, **(D)** hypothalamus, **(E)** amygdala and **(F)** plasma. **(G)** Plasma corticosterone levels. Data are expressed as mean ± SEM. *$p<0.05$, **$p<0.01$, ***$p<0.001$ Two-way ANOVA followed by LSD *post-hoc* test. *Abbreviations*: AcbC, nucleus accumbens core; AcbSh, nucleus accumbens shell; Amy, amygdala; AOL, anterior olfactory nucleus-lateral; AOM, anterior olfactory nucleus-medial; AOV, anterior olfactory nucleus-ventral; CgCx, cingulate cortex; CPu, caudate-putamen; Hip, hippocampus; Hyp, hypothalamus; LS, lateral septum; MS, medial septum; OT, oxytocin; OTR, oxytocin receptor; Pir, piriform cortex; Th, thalamus; VDB, vertical limb of the diagonal band of Broca.

Figure 5: Effect of chronic methamphetamine administration and withdrawal on [^{3}H]DAMGO binding to MOPr and [^{3}H]Raclopride binding to D_2R . Male C57BL/6J mice were treated either with

saline or methamphetamine (METH) with a 10-day steady-dose administration paradigm (2 mg/kg, i.p. per day) and left to spontaneously withdraw for a period of 7 days. (**A)** Computer-enhanced representative MOPr autoradiograms of adjacent coronal brain sections from chronic saline-, METH-treated, saline-withdrawn and METH-withdrawn mice at the level of the caudate putamen (Bregma 0.86mm). MOPrs were labelled with [^{3}H]DAMGO (4nM). The color bar illustrates a pseudo-color interpretation of black and white film images in fmol/mg tissue equivalent. **(B)** Quantitative MOPr autoradiographic binding in brain regions of mice treated and withdrawn form METH. **(C)** Computer-enhanced representative D_2R autoradiograms of adjacent coronal brain sections from chronic saline-, METH-treated, saline-withdrawn and METH-withdrawn mice at the level of the caudate putamen (Bregma 0.86mm). D_2R were labelled with [^{3}H]-Raclopride (4nM). The color bar illustrates a pseudo-color interpretation of black and white film images in fmol/mg tissue equivalent. **(D)** Quantitative D_2R autoradiographic binding in brain regions of mice treated and withdrawn form METH. Data are expressed as mean ± SEM. Two-way ANOVA was performed in each individual brain region. *Abbreviations*: AcbC, nucleus accumbens core; AcbSh, nucleus accumbens shell; Amy, amygdala; CgCx, cingulate cortex; CPu, caudate-putamen; D_2R, dopamine D_2 receptor; Hip, hippocampus; Hyp, hypothalamus; LS, lateral septum; MS, medial septum; MOPr, μ-opioid receptor; MtCx, motor cortex; Pir, piriform cortex; Th, thalamus; VDB, vertical limb of the diagonal band of Broca.

Figure 6: Effect of chronic METH administration and withdrawal on CRF$^+$, c-Fos$^+$ and c-Fos$^+$/CRF$^+$ neurons in the amygdala. Male C57BL/6J mice were treated either with saline or methamphetamine (METH) with a 10-day steady-dose administration paradigm (2 mg/kg, i.p. per day) and left to spontaneously withdraw for a period of 7 days. Representative immunohistochemical images of c-Fos$^+$/CRF$^+$ neurons from the amygdala from chronic **(A**) saline-, **(B)** METH-treated, **(C)** saline-withdrawn and **(D)** METH-withdrawn mice (Scale bar: 200μm). Quantitative immunohistochemical analysis of **(E)** CRF$^+$, **(F)** c-Fos$^+$ and **(G)** c-Fos$^+$/CRF$^+$ neurons in the amygdala of mice treated with a 10-day steady-dose METH administration paradigm and in mice-withdrawn for 7 days. Data are expressed

as mean ± SEM. *$p<0.05$, **$p<0.01$, ***$p<0.001$. Two-way ANOVA followed by LSD *post-hoc* test. CRF, corticotropin-releasing factor.

A ***Experiment 1:*** **Behavioural characterisation**

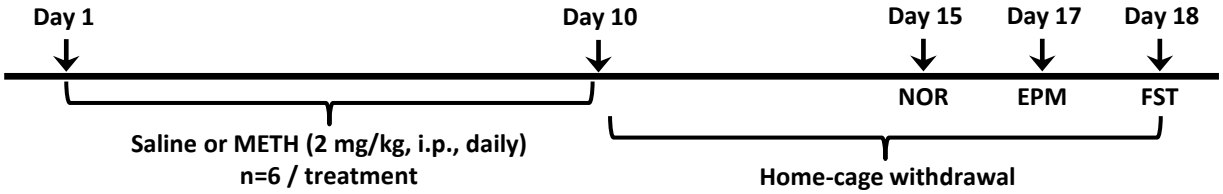

B ***Experiment 2:*** **Locomotor and stereotypic rearing activity**

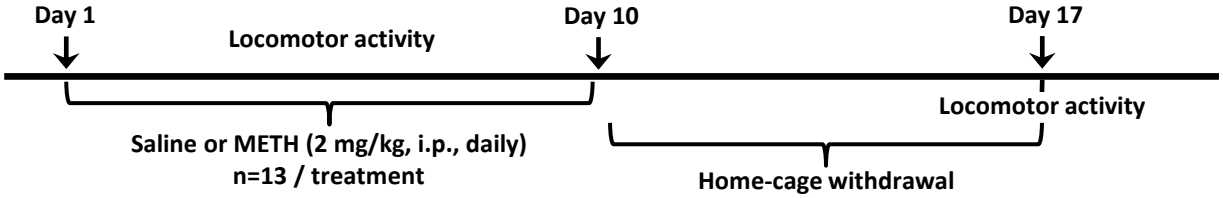

C ***Experiment 3:*** **OTR, MOPr, D_2R, CRF and plasma corticosterone measurements**

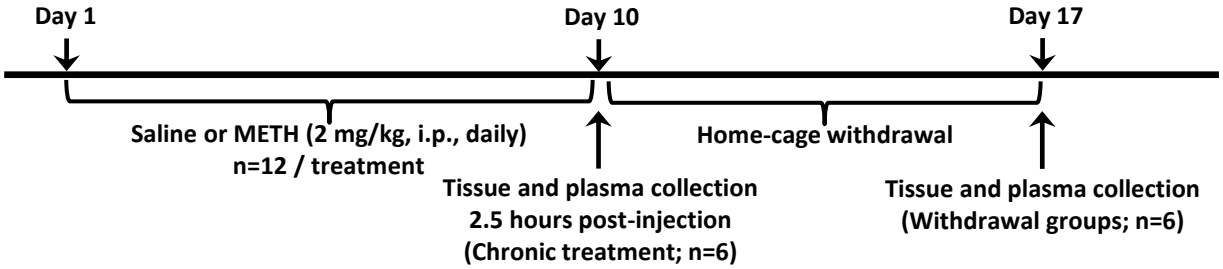

D ***Experiment 4:*** **Brain and plasma OT measurements**

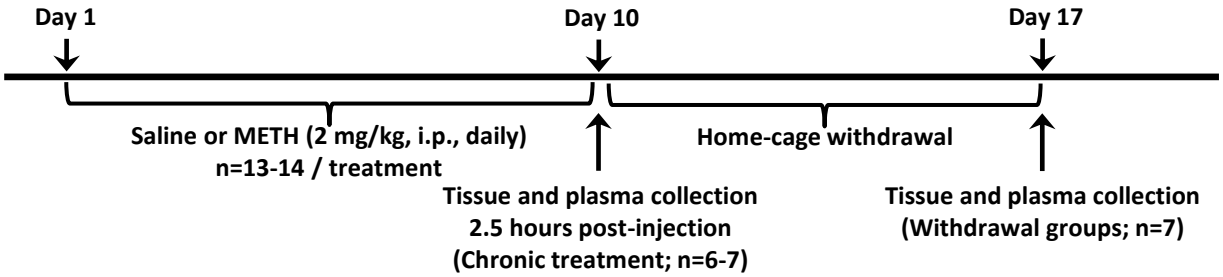

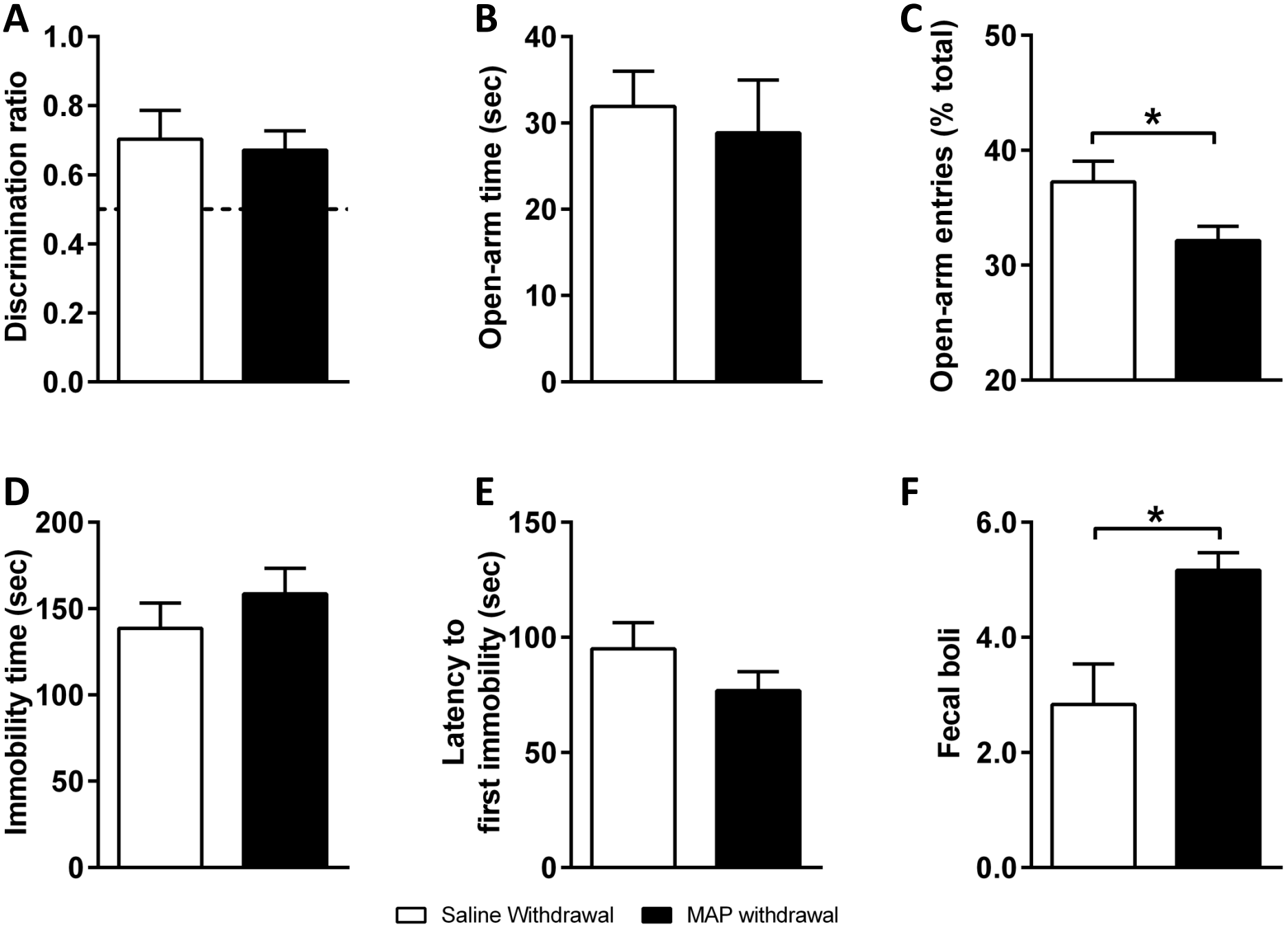
A
Discrimination ratio
1.0
0.8
0.6
0.4
0.2
0.0
B
Open-arm time (sec)
40
30
20
10
0
C
Open-arm entries (% total)
50
40
30
20
*
D
Immobility time (sec)
200
150
100
50
0
E
Latency to first immobility (sec)
150
100
50
0
F
Fecal boli
6.0
4.0
2.0
0.0
*
Saline Withdrawal
MAP withdrawal

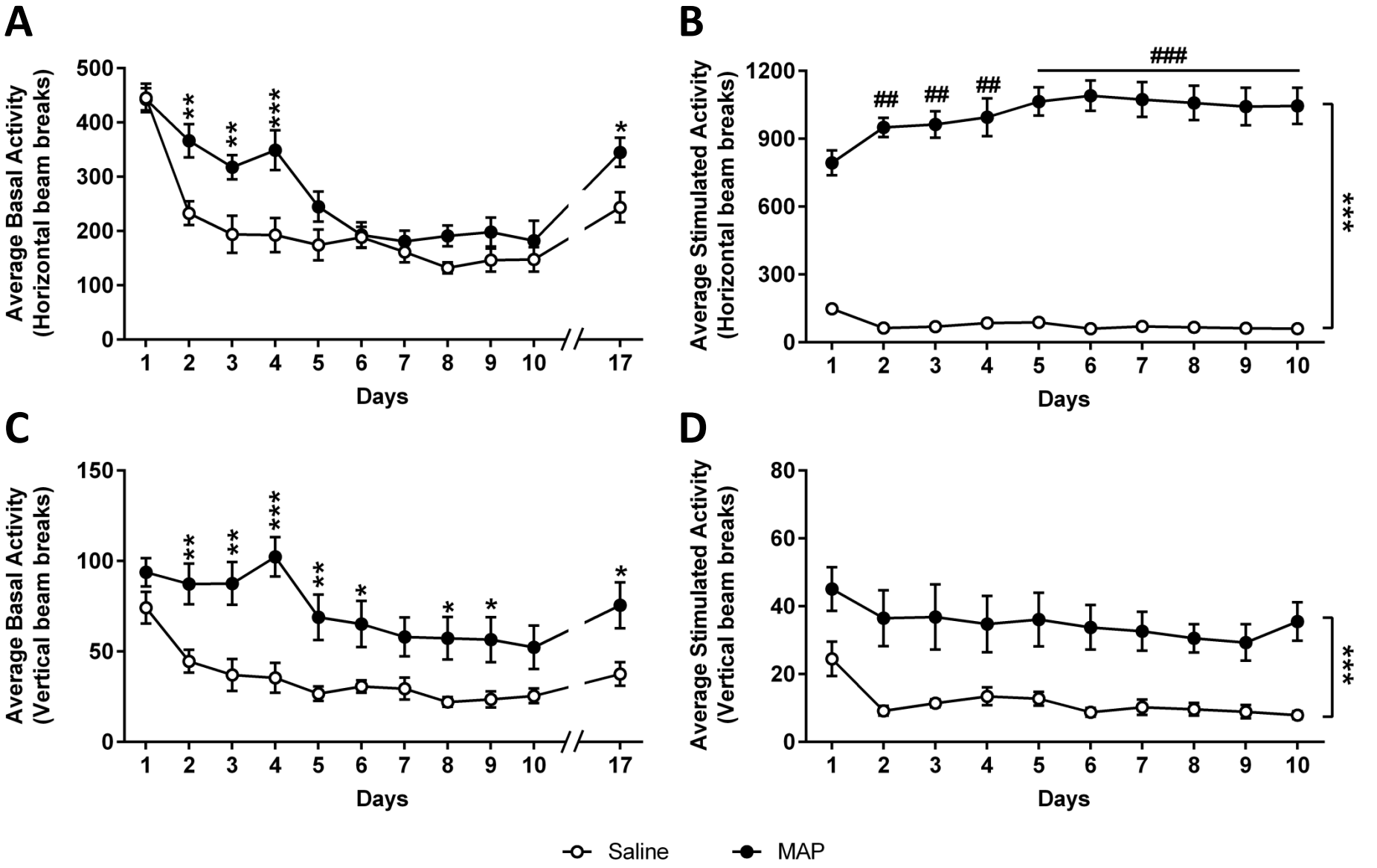
A
Average Basal Activity
(Horizontal beam breaks)
500
400
300
200
100
0
1 2 3 4 5 6 7 8 9 10 17
Days
B
Average Stimulated Activity
(Horizontal beam breaks)
1200
900
600
300
0
1 2 3 4 5 6 7 8 9 10
Days
C
Average Basal Activity
(Vertical beam breaks)
150
100
50
0
1 2 3 4 5 6 7 8 9 10 17
Days
D
Average Stimulated Activity
(Vertical beam breaks)
80
60
40
20
0
1 2 3 4 5 6 7 8 9 10
Days
Saline
MAP

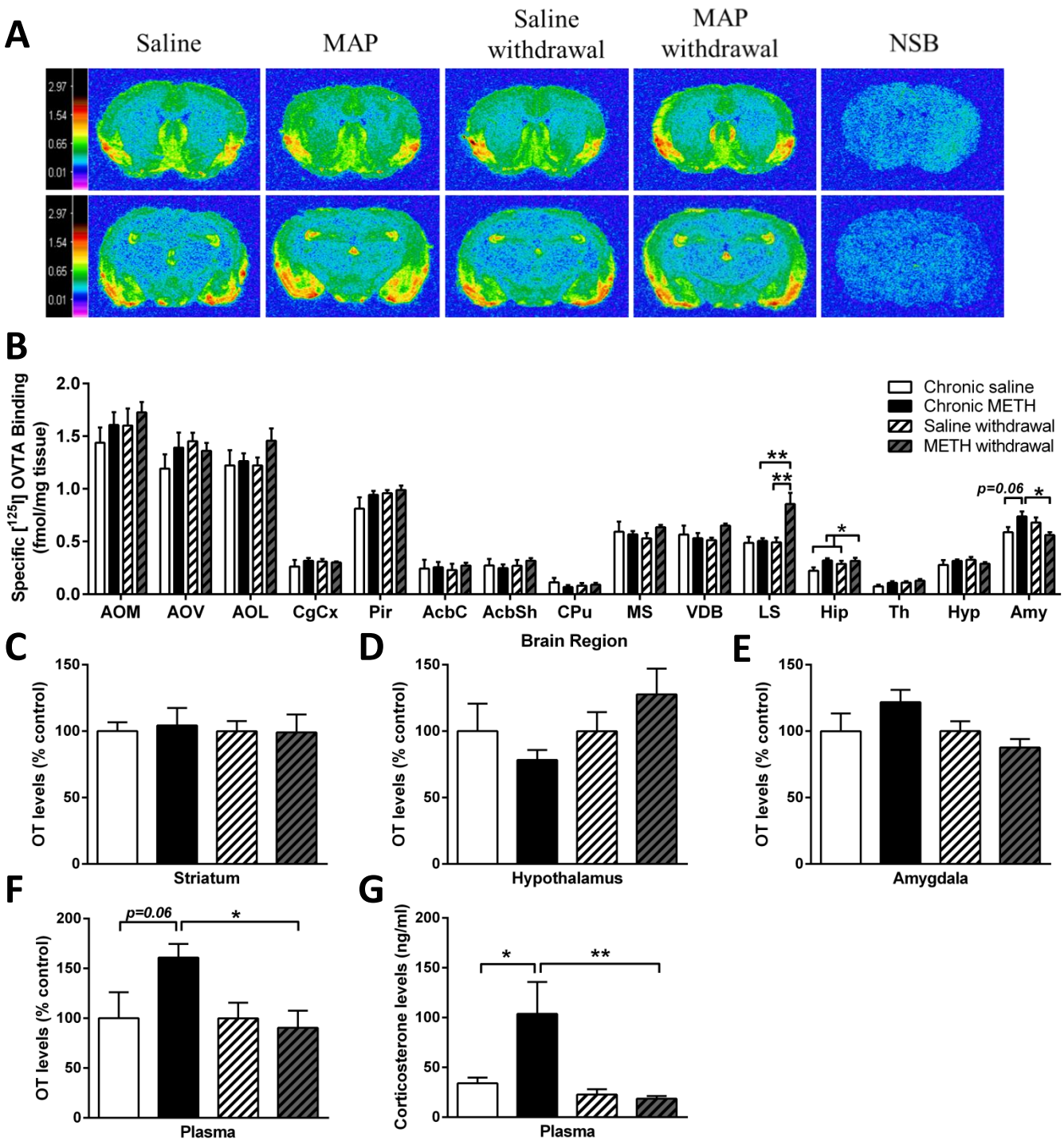
A
Saline
MAP
Saline withdrawal
MAP withdrawal
NSB
2.97
1.54
0.65
0.01
B
Specific [125I] OVTA Binding (fmol/mg tissue)
Chronic saline
Chronic METH
Saline withdrawal
METH withdrawal
AOM
AOV
AOL
CgCx
Pir
AcbC
AcbSh
CPu
MS
VDB
LS
Hip
Th
Hyp
Amy
p=0.06
C
OT levels (% control)
Striatum
D
Brain Region
Hypothalamus
E
Amygdala
F
Plasma
G
Corticosterone levels (ng/ml)
Plasma

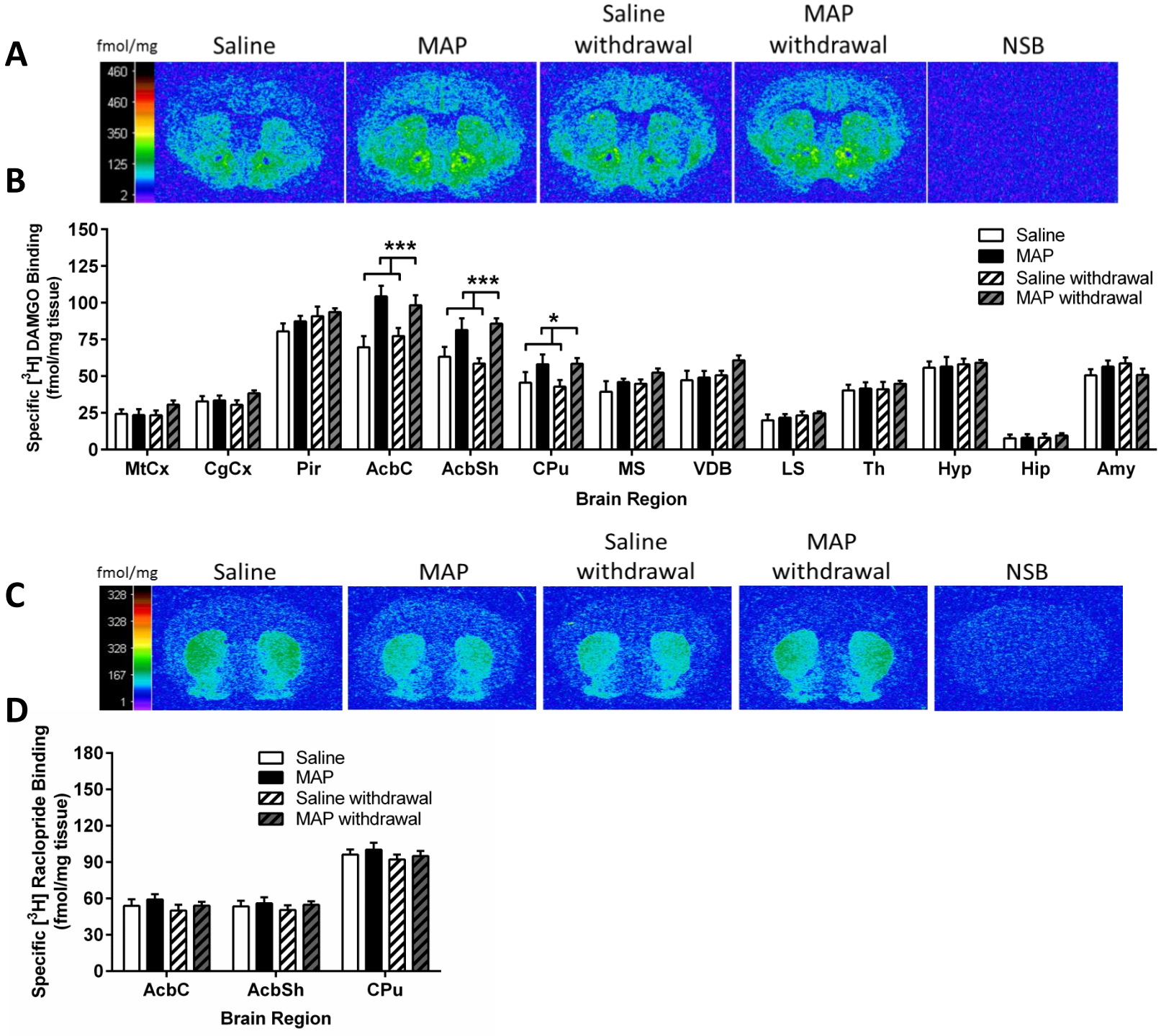
A
fmol/mg
460
460
350
125
2
Saline
MAP
Saline withdrawal
MAP withdrawal
NSB
B
Specific [3H] DAMGO Binding (fmol/mg tissue)
150
125
100
75
50
25
0
***
***
*
Saline
MAP
Saline withdrawal
MAP withdrawal
MtCx
CgCx
Pir
AcbC
AcbSh
CPu
MS
VDB
LS
Th
Hyp
Hip
Amy
Brain Region
C
fmol/mg
328
328
328
167
1
Saline
MAP
Saline withdrawal
MAP withdrawal
NSB
D
Specific [3H] Raclopride Binding (fmol/mg tissue)
180
150
120
90
60
30
0
Saline
MAP
Saline withdrawal
MAP withdrawal
AcbC
AcbSh
CPu
Brain Region

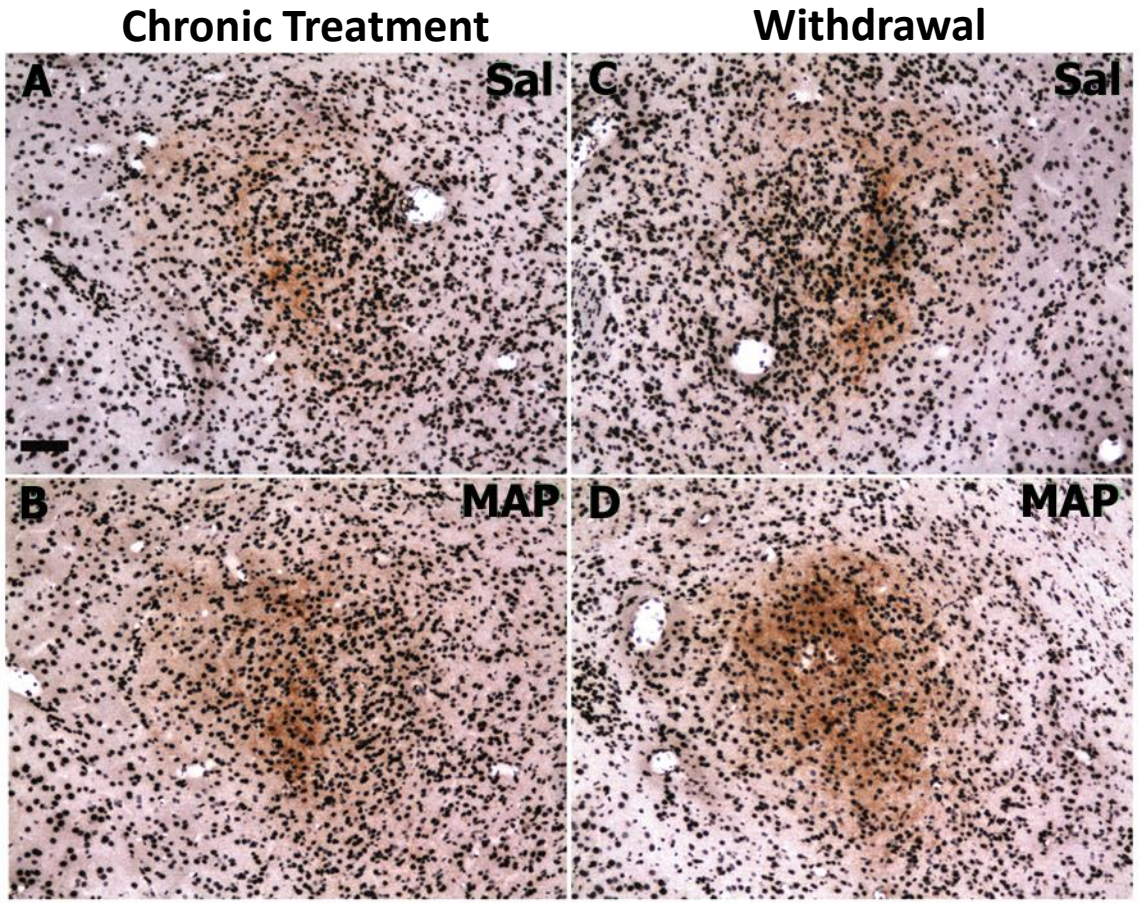
Chronic Treatment
Withdrawal
A
Sal
C
Sal
B
MAP
D
MAP

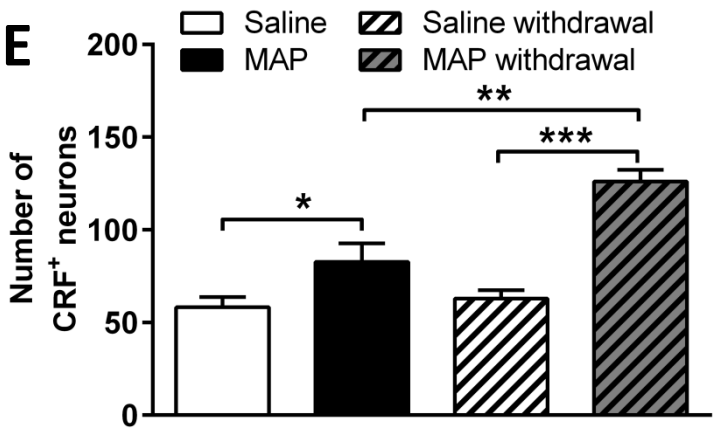
E
Saline
MAP
Saline withdrawal
MAP withdrawal
Number of CRF+ neurons
200
150
100
50
0
*
**
***

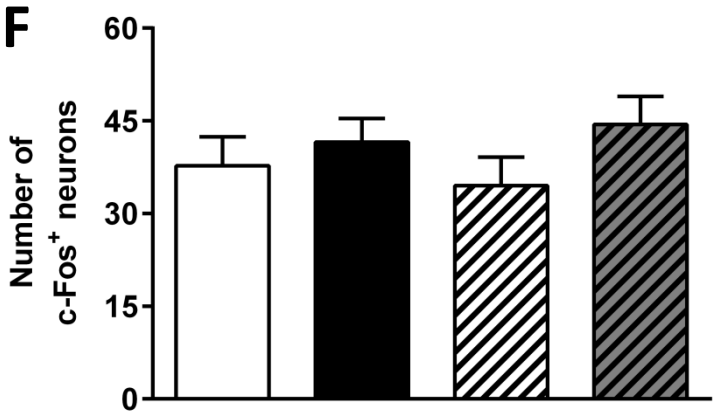
F
Number of c-Fos+ neurons
60
45
30
15
0

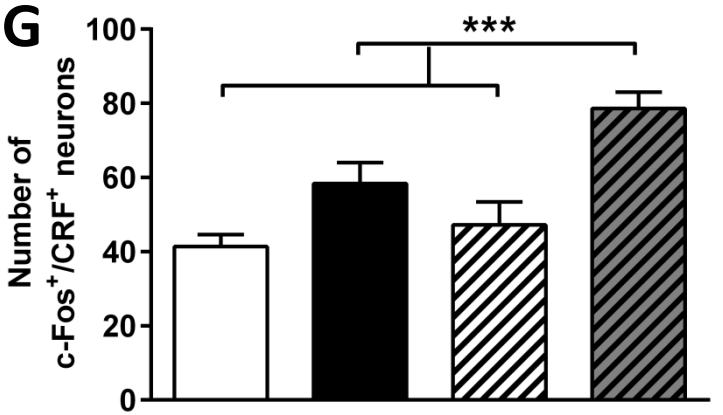
G
Number of c-Fos+/CRF+ neurons
100
80
60
40
20
0
***

Highlights:

- METH withdrawal induces anxiety-related symptoms in mice
- METH administration and withdrawal causes neuroadaptations in the OT system
- Persistent increase in striatal MOPr following METH treatment
- Amygdalar c-Fos^{+}/CRF^{+} neurons are increased in METH-treated/withdrawn mice

Role of funding sources

Funding for this study was provided by a Royal Society grant (RG120556; P.I. Alexis Bailey) and by Lilia and Charalambos Georgiou. JAGC was in receipt of a pre-doctoral fellowship from Fundación Séneca, Agencia de Ciencia y Tecnología de la Región de Murcia (15519/FPI/10). The sponsors had no involvement in the design of the study and in the collection, analyses and interpretation of the data, nor in the writing of the manuscript and the decision to submit this article for publication.

Conflict of interest

The authors declare no conflict of interest.